

quency independent and take following values:

$$R_1^B = 1.68, \quad R_2^B = 0.75,$$

$$R_3^B = 0.98, \quad R_4^B = 1.14,$$

where superscript *B* refers to the Born approximation. If, on the other hand, we take into account the higher-order rescattering effects, the partition ratios decrease considerably and give the values rather smaller than unity, as is seen in Figs. 5(a) and 5(b). These characteristic results are completely consistent with the results obtained in Ref. 7, in which only two modes, *R* and *T*, were involved. Moreover, it is noteworthy that there appears no resonance in the scattering process

$$R + \Delta M \rightarrow SH + \Delta M.$$

In conclusion, we have investigated the scattering of elastic surface waves from static point-mass defect localized in the solid surface by solving approximately the so-called Chew-Low equation. We would like to emphasize the following two points. First, resonance structure appears in all the cross sections but  $\sigma_{R-SH}$  for a static surface defect of lighter mass than that of the host atoms. Second, the inclusion of the rescattering effects of elastic surface waves with mass defect appreciably enhances the scattering into other Rayleigh-mode waves.

The numerical calculations were performed using a FACOM 230-60 computer at the Computer Center of Hokkaido University.

- <sup>1</sup>H. Ezawa, T. Kuroda, and K. Nakamura, *Surf. Sci.*, **24**, 654 (1971); H. Ezawa, S. Kawaji, T. Kuroda, and K. Nakamura, *Surf. Sci.*, **24**, 649 (1971); H. Ezawa, S. Kawaji, and K. Nakamura, *Surf. Sci.*, **27**, 218 (1971); S. Kawaji, H. Ezawa, and K. Nakamura, *International Conference on Solid Surface*, Boston, 1971 (unpublished); *J. Vac. Sci. Technol.*, **9**, 762 (1972).  
<sup>2</sup>H. Ezawa, *Ann. Phys.*, **67**, 438 (1971). In this article, Ezawa named the quantum of elastic surface waves "surfon."  
<sup>3</sup>R. G. Steg and P. G. Klemens, *Phys. Rev. Lett.*, **24**, 381 (1970).  
<sup>4</sup>S. Takeno, *Prog. Theor. Phys.*, **29**, 191 (1963); M. V.

- Klein, *Phys. Rev.*, **131**, 1500 (1963); J. Callaway, *Nuovo Cimento*, **29**, 883 (1963); R. J. Elliot and D. W. Taylor, *Proc. Phys. Soc.*, **83**, 189 (1964); J. A. Krumhansl, in *Proceedings of the International Conference on Lattice Dynamics, Copenhagen*, 1963, edited by R. F. Wallis (Pergamon, Oxford, England, 1965), p. 523; M. Yussouff and J. Mahanty, *Proc. Phys. Soc.*, **85**, 1223 (1965); B. K. Agarwal, *J. Phys.*, **2**, 252 (1969).  
<sup>5</sup>M. Ashkin, *Phys. Rev.*, **136**, B821 (1964).  
<sup>6</sup>T. Nakayama and T. Sakuma, *Lett. Nuovo Cimento*, **2**, 1104 (1971).  
<sup>7</sup>T. Sakuma, *Phys. Rev. Lett.*, **29**, 1394 (1972).  
<sup>8</sup>G. F. Chew and F. E. Low, *Phys. Rev.*, **101**, 1570 (1956).

## Molecular-Orbital Studies of $As_2S_3$ and $As_2Se_3$

Inan Chen

Xerox Rochester Research Center, Rochester, New York 14644

(Received 12 February 1973)

The basis hybrid orbitals of  $As_2S_3$  and  $As_2Se_3$  for the molecular-orbital calculation of the layer molecules have been investigated. One feature distinct from and one similar to amorphous Se is observed. The former is the inequivalence of the nearest-neighbor  $\sigma$  bonds, which can be interpreted as a reason for low carrier mobilities in these solids. The similar feature is the locations of the bonding and the lone-pair states. As in Se, these are intermixed; thus band-gap photons can break  $\sigma$  bonds, which accounts for the photodissociation and photocrystallization of chalcogenide glasses.

### I. INTRODUCTION

In a recent paper<sup>1</sup> the electronic states of a molecular solid—amorphous selenium—has been successfully interpreted by molecular-orbital (MO) theory. In that paper, the calculation of the electronic states of the solid is carried out in three steps. The first step is the identification of the building block, or the basis orbitals for the molecular states. The second step is the calculation of the molecular orbitals by a semiempirical (extend-

ed Hueckel) method,<sup>2</sup> including as many units as the convergence requires. Finally, the electronic density of states in the solid is calculated by assuming a Gaussian distribution of states centered at the molecular states. It is found that the first step has a determinate effect on the density of states in the solids, e.g., only when the bonding and antibonding orbitals between two neighboring atoms, and the lone-pair hybrid orbitals are chosen as bases for the MO calculations, the calculated density of states agrees with that obtained from

photoemission experiment.<sup>3</sup> When atomic orbitals are chosen as the bases, the calculated width of valence band was more than twice the observed value.

The calculation also gives a new interpretation to the origin of the double peaks in the density of states and the reflectivity spectra. It was suggested that the two peaks represent the contributions from the states arising from the lone-pair orbitals and those from the bonding orbitals, respectively.<sup>4,5</sup> On the contrary, the new analysis<sup>1</sup> reveals that the origins of the two peaks cannot be associated with any particular type of basis orbitals. In the process of forming a molecule (chain), both the lone-pair orbitals and the bonding orbitals split into two groups of states, one being stabilized and the other antistabilized with respect to the basis-orbital energy. Since the basis-orbital energies of the lone-pair and the bonding orbitals are very close, and the interaction energies between two neighboring units are all of the same order of magnitude, the stabilized, as well as the antistabilized, group of states arising from the lone pairs overlaps that from the bonding orbitals. Thus the two peaks represent contributions from the antistabilized and the stabilized groups of states, respectively.

Arsenic trisulfide ( $As_2S_3$ ) and arsenic triselenide ( $As_2Se_3$ ) form molecular solids of semi-infinite "molecules" similar to selenium, except that the "molecule" is a layer rather than a chain as in the latter (Fig. 1). In principle, the electronic states of  $As_2S_3$  ( $As_2Se_3$ ) can be calculated by the same approach described above. However, because the layer "molecule" extends in two dimensions (compared to the one-dimensional extension of Se chain), the second step in the calculation becomes extremely time consuming. On the other hand, as demonstrated by the calculation on selenium,<sup>1</sup> the essence of the electronic structure lies in the first step of the calculation, which involves much simpler computations.

In the present paper, we shall calculate the basis orbitals and their energies for  $As_2S_3$  and  $As_2Se_3$  and show that we can expect the same situation regarding the lone-pair and bonding states as in selenium.

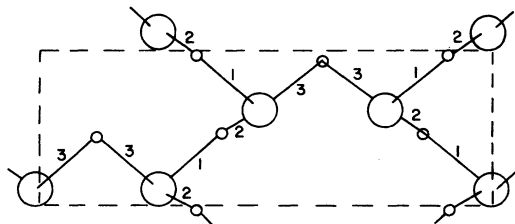


FIG. 1. Unit-cell structure of  $As_2S_3$  and  $As_2Se_3$  in  $ac$  plane, approximate scale; the large circles represent As, the small ones S (Se). Types of  $\sigma$  bonds are indicated.

TABLE I. Hybrid orbitals of  $As_2S_3$ .

	$s$	$p_x$	$p_y$	$p_z$	$E(eV)$
As $\sigma_1$	0.551	0.561	-0.231	0.573	-11.65
$\sigma_2$	0.171	0.450	0.835	-0.268	-9.30
$\sigma_3$	0.380	-0.671	0.434	0.466	-10.28
$\lambda_A$	0.723	-0.181	-0.249	-0.618	-13.53
$S_1$ $\sigma_1$	0.453	-0.599	0.247	-0.612	-13.52
$\sigma_2$	0.453	0.407	0.755	0.242	-13.52
$\lambda_1$	0.543	-0.401	-0.322	0.664	-14.32
$\lambda_2$	0.543	0.561	-0.515	-0.354	-14.32
$S_3$ $\sigma_3$	0.223	$\pm 0.707$	-0.457	-0.491	-12.11
$\lambda_3$	0.671	0.0	-0.366	0.645	-15.73
$\lambda'_3$	0.671	0.0	0.670	-0.318	-15.73
VSIE: As $E_s = -17.605$ eV, $E_p = -9.050$ eV					
S $E_s = -20.704$ eV, $E_p = -11.654$ eV					

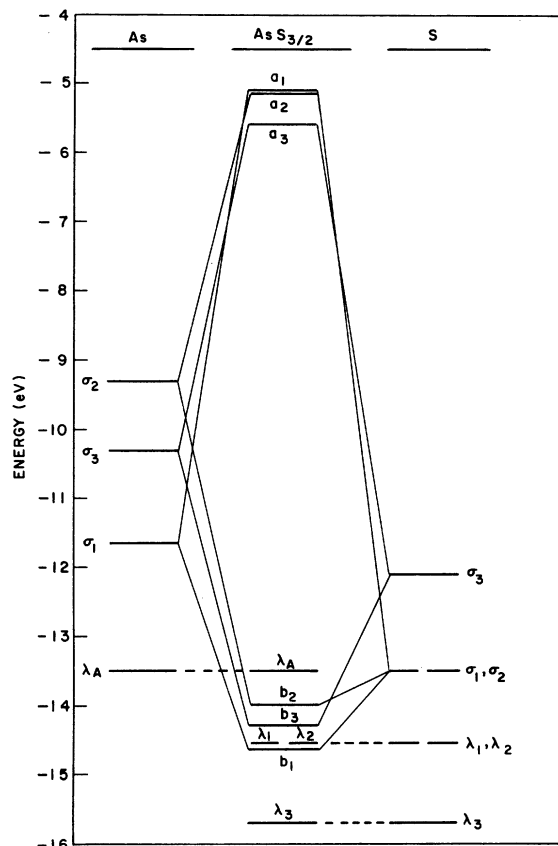
These results will be used to interpret the photo-decomposition and photocrystallization of chalcogenide glasses.<sup>6-8</sup> Also a feature distinct from selenium will be pointed out and the possible consequences for carrier transport will be discussed.

## II. RESULTS AND DISCUSSION

The  $\sigma$  and lone-pair hybrid orbitals of As, S, and Se atoms are determined by the method described in the Appendix, from the crystal-structure data of  $As_2S_3$  and  $As_2Se_3$  (Fig. 1).<sup>9,10</sup> The As atoms are all equivalent but there are two inequivalent S (Se) atoms. The hybrid orbitals and their energies are given in Tables I and II. The signs of the coefficients of  $p_x$ ,  $p_y$ , and  $p_z$  depend on the position of the atom in the unit cell, but these are irrelevant to our discussion here. Only the absolute values which determine the hybrid energy and the composition are important. The energies are calculated from the valence-state ionization energies (VSIE)<sup>11</sup> of the atomic orbitals shown at the bottom of the tables.

TABLE II. Hybrid orbitals of  $As_2Se_3$ .

	$s$	$p_x$	$p_y$	$p_z$	$E(eV)$
As $\sigma_1$	0.644	0.537	-0.251	0.483	-12.60
$\sigma_2$	0.169	0.425	0.852	-0.255	-9.30
$\sigma_3$	0.293	-0.649	0.431	0.554	-9.79
$\lambda_A$	0.686	-0.332	-0.159	-0.628	-13.08
$Se_1$ $\sigma_1$	0.393	-0.646	0.302	-0.581	-12.34
$\sigma_2$	0.393	0.397	0.795	0.238	-12.34
$\lambda_1$	0.588	-0.371	-0.301	0.653	-14.26
$\lambda_2$	0.588	0.537	-0.432	-0.424	-14.26
$Se_3$ $\sigma_3$	0.271	0.653	$\pm 0.434$	$\pm 0.558$	-11.52
$\lambda_3$	0.653	-0.271	$\pm 0.558$	$\mp 0.434$	-15.07
VSIE: As $E_s = -17.605$ eV, $E_p = -9.050$ eV					
Se $E_s = -20.828$ eV, $E_p = -10.786$ eV					

FIG. 2. Energy-level scheme for  $\text{AsS}_{3/2}$ .

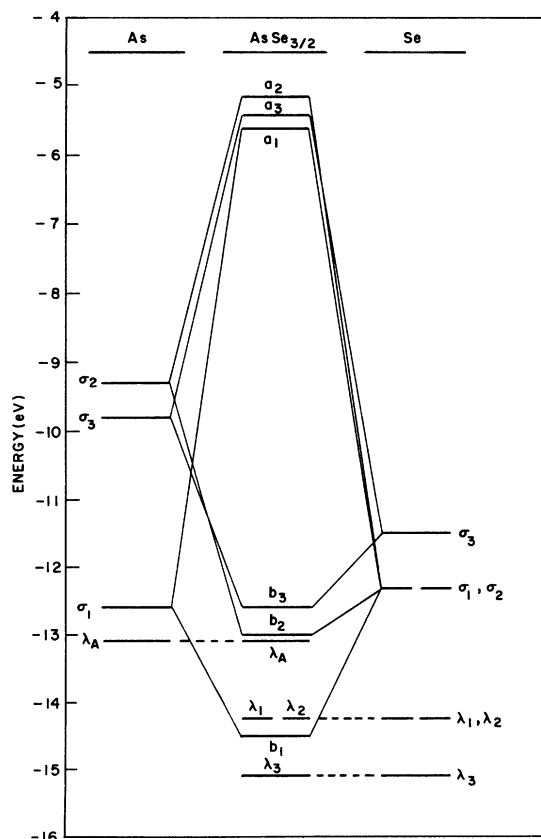
The covalent bonds are formed between  $\sigma$  hybrids of As and S (Se), with the same subscripts. The resulting bonding ( $b$ ) and antibonding ( $a$ ) orbital energies are calculated by the semiempirical method<sup>2,11,12</sup> using Cusachs's<sup>13</sup> empirical formula for the off-diagonal elements of Hamiltonian matrix. The results are illustrated in Figs. 2 and 3. The hybrid orbital energies of As and S (Se) are shown on the left- and the right-hand sides of Fig. 2 (Fig. 3), respectively. The center column shows the orbital energy levels of a fictitious molecule  $\text{AsS}_{3/2}$  ( $\text{AsSe}_{3/2}$ ). These orbitals would be the bases for calculating the molecular orbitals of a layer "molecule."

The three As-S (As-Se) bonds are quite asymmetric. This can be expected from the hybrid coefficients in Tables I and II, and is a feature distinct from Se chain and groups IV, II-VI, and III-V covalent solids in which all the covalent bonds are equivalent. Because of this asymmetry the nearest-neighbor bonds of types 1 and 2 are not degenerate in energy, it is the next-nearest-neighbor bonds (see Fig. 1) which are degenerate. For the type-3 bonds one of the nearest neighbors is degenerate,<sup>14</sup> but such degenerate pairs are separated by more than 5 Å. Thus the interactions between the bond-

ing orbitals in the "molecule" are considerably weaker than those in other covalent solids. From this weaker interaction one can expect more localized states or narrower bands, resulting in lower carrier mobilities; e.g., the hole mobility is  $4 \times 10^{-5} \text{ cm}^2/\text{V sec}$  at  $10^5 \text{ V/cm}$  in amorphous  $\text{As}_2\text{Se}_3$ , while it is  $0.1 \text{ cm}^2/\text{V sec}$  in amorphous Se.<sup>15</sup> The asymmetry may be slightly relaxed in the amorphous states.

A feature similar to amorphous Se is the locations of the bonding-orbital and the lone-pair-orbital levels. These are intermixed in an energy range of  $\sim 2.5 \text{ eV}$ . Thus if we had carried out the MO and the density-of-state calculations (steps 2 and 3), we would find both the bonding and the lone-pair orbitals contributing to the upper valence band, as in the case of amorphous Se.

Berkes, Ing, and Hillegas<sup>6</sup> have reported the photodissociation of amorphous  $\text{As}_2\text{S}_3$  and  $\text{As}_2\text{Se}_3$ , and Dresner and Stringfellow,<sup>7</sup> and Feinleib *et al.*<sup>8</sup> have reported photoinduced crystallization of other chalcogenide glasses, all with photons of band-gap energies. These phenomena are attributed to the breaking of the  $\sigma$  bonds by the photon. However, according to the classical picture<sup>4,5</sup> in chalcogenide solids the bonding-orbital states are well separated

FIG. 3. Energy-level scheme for  $\text{AsSe}_{3/2}$ .

from and lie lower in energy than the lone-pair states, the band-gap energy light cannot break a  $\sigma$  bond. The new energy-level scheme of the present calculation (Figs. 2 and 3) revises this picture, and now the bond-breaking model of photodissociation and photocrystallization can be accounted for.

#### APPENDIX: HYBRID ORBITALS OF $As_2S_3$ AND $As_2Se_3$

The  $4s$ ,  $4p$  atomic orbitals of As and the  $3s$ ,  $3p$  ( $4s$ ,  $4p$ ) atomic orbitals of S (Se) are hybridized into directed bonds ( $\sigma$ ) and lone pairs as follows.

For the As atom, there are three  $\sigma$  and one lone-pair hybrids. They can be represented as

$$\sigma_i = \alpha_i s + (1 - \alpha_i^2)^{1/2} p_i, \quad i = 1, 2, 3 \quad (A1)$$

$$\lambda = \alpha_4 s + (1 - \alpha_4^2)^{1/2} p_4, \quad (A2)$$

where  $p_i$  is a combination of  $p_x$ ,  $p_y$ , and  $p_z$  orbitals:

$$p_i = \xi_i p_x + \eta_i p_y + \zeta_i p_z. \quad (A3)$$

Let the coordinates of As atom be  $(x_0, y_0, z_0)$  and the three bonding neighbor S (Se) atoms be at  $(x_i, y_i, z_i)$ ,  $i = 1, 2, 3$ ; then

$$\xi_i = (x_i - x_0)/R_i,$$

$$\eta_i = (y_i - y_0)/R_i, \quad i = 1, 2, 3 \quad (A4)$$

$$\zeta_i = (z_i - z_0)/R_i,$$

where  $R_i$  is the bond length,

$$R_i = [(x_i - x_0)^2 + (y_i - y_0)^2 + (z_i - z_0)^2]^{1/2}. \quad (A5)$$

The orthogonality among the three  $\sigma$  hybrids gives

$$\alpha_i \alpha_j + (1 - \alpha_i^2)^{1/2} (1 - \alpha_j^2)^{1/2} C_{ij} = 0, \quad i, j = 1, 2, 3 \quad (A6)$$

where the cosine of the bond angle  $C_{ij}$  is given by

$$C_{ij} = \xi_i \xi_j + \eta_i \eta_j + \zeta_i \zeta_j. \quad (A7)$$

Equation (A6) gives three relations for the determinations of  $\alpha_i$ ,  $i = 1, 2, 3$ . The result is

$$\alpha_i^2 = C_{ij} C_{ik} / (C_{jk} - C_{ij} C_{ik}), \quad (A8)$$

where  $i, j, k$  are permutations of 1, 2, and 3.

It now remains the determination of  $p_4$ . The orthogonality of  $\lambda$  and  $\sigma_i$  gives the following simultaneous linear equations for  $\xi_4$ ,  $\eta_4$ , and  $\zeta_4$ :

$$\xi_i \xi_4 + \eta_i \eta_4 + \zeta_i \zeta_4 = - \frac{\alpha_i \alpha_4}{(1 - \alpha_i^2)^{1/2} (1 - \alpha_4^2)^{1/2}}, \quad (A9)$$

$$i = 1, 2, 3$$

where  $\alpha_4$  is given by the normalization of  $s$  orbital,

as

$$\alpha_4 = \left( 1 - \sum_{i=1}^3 \alpha_i^2 \right)^{1/2}.$$

For the S (Se) atom, there are two  $\sigma$  and two lone-pair orbitals. Without loss of generality we may assume that the two  $\sigma$ , as well as the two lone pairs are equivalent to each other, i. e., have the same  $s$  components. Then

$$\sigma_i = \alpha s + (1 - \alpha^2)^{1/2} p_i, \quad i = 1, 2 \quad (A10)$$

$$\lambda_j = (\frac{1}{2} - \alpha^2)^{1/2} s + (\frac{1}{2} + \alpha^2)^{1/2} p_j, \quad j = 3, 4. \quad (A11)$$

As in the case of As  $\sigma$  orbitals,  $p_i$  ( $i = 1, 2$ ) can be determined from the coordinates of the S (Se) atom and the bonded neighbor As atoms, Eqs. (A3)–(A5). The  $s$  component of the  $\sigma$  orbital,  $\alpha$ , is determined from the cosine of the bond angle and the orthogonality relation between the two  $\sigma$ 's:

$$\alpha^2 = -C_{12} / (1 - C_{12}). \quad (A12)$$

The orthogonality between the  $\sigma$ 's and the lone pair give the following relation:

$$\xi_i \xi + \eta_i \eta + \zeta_i \zeta = \frac{-\alpha (\frac{1}{2} - \alpha^2)^{1/2}}{(1 - \alpha^2)^{1/2} (\frac{1}{2} + \alpha^2)^{1/2}}, \quad (A13)$$

$$i = 1, 2$$

where  $\xi$ ,  $\eta$ ,  $\zeta$  are the coefficients in  $p_j$  ( $j = 3, 4$ ).  $\xi$  and  $\eta$  can be solved in terms of  $\zeta$  from the two equations, Eq. (A13) and substituted into the normalization relation

$$\xi^2 + \eta^2 + \zeta^2 = 1. \quad (A14)$$

This yields a quadratic equation for  $\zeta$ , which can be solved numerically for two sets of  $\xi$ ,  $\eta$ ,  $\zeta$  values for the two lone pairs.

The hybrid orbitals of As and S atoms in  $As_2S_3$  determined from the atomic positions in the unit cell<sup>9</sup> are given in Table I. The hybrid orbital energy  $E_h$  is given by

$$E_h = \alpha^2 E_s + (1 - \alpha^2) E_p, \quad (A15)$$

where  $\alpha$  is the coefficient of the  $s$  orbital and  $E_s$  and  $E_p$  are the valence state ionization energies of the  $s$  and  $p$  orbitals, respectively. For  $As_2Se_3$ , two of the Se bond angles are reported<sup>10</sup> to be less than  $90^\circ$ . Strictly speaking, such cases cannot be represented by  $sp$  hybrids. However, since the difference is very small ( $4^\circ$ ) we have approximated the angles as  $90^\circ$ . The results are given in Table II.

<sup>1</sup>I. Chen, Phys. Rev. B 7, 3672 (1973).

<sup>2</sup>M. D. Newton, F. P. Boer, and W. N. Lipscomb, J. Am. Chem. Soc. 88, 2353 (1966); L. C. Cusachs and B. B. Cusachs, J. Phys. Chem. 71, 1060 (1967); R. P. Messmer and G. D. Watkins, Phys. Rev. Lett. 25, 656 (1970); Phys. Rev. Lett. 27, 1573

(1971).

<sup>3</sup>P. Nielsen, Phys. Rev. B 6, 3739 (1972).

<sup>4</sup>M. Kastner, Phys. Rev. Lett. 28, 355 (1972).

<sup>5</sup>R. E. Drews, R. L. Emerald, M. L. Slade, and R. Zallen, Solid State Commun. 10, 293 (1972).

- <sup>6</sup>J. S. Berkes, S. W. Ing, Jr., and W. J. Hillegas, *J. Appl. Phys.* **42**, 4908 (1971).  
<sup>7</sup>J. Dresner and G. B. Stringfellow, *J. Phys. Chem. Solids* **29**, 303 (1968).  
<sup>8</sup>J. Feinleib, J. deNeufville, S. C. Moss, and S. R. Ovshinsky, *Appl. Phys. Lett.* **18**, 254 (1971).  
<sup>9</sup>N. Morimoto, *Mineral. J. (Sapporo)* **1**, 160 (1954).  
<sup>10</sup>A. A. Vaipolin, *Kristallografiya* **10**, 596 (1965) [*Sov. Phys.-Crystallogr.* **10**, 509 (1966)].

- <sup>11</sup>C. J. Ballhausen and H. B. Gray, *Molecular Orbital Theory* (Benjamin, New York, 1964), p. 120.  
<sup>12</sup>M. Wolfsberg and L. Helmholz, *J. Chem. Phys.* **20**, 837 (1952).  
<sup>13</sup>L. C. Cusachs, *J. Chem. Phys. Suppl.* **43**, S157 (1965).  
<sup>14</sup>This degeneracy is based on the layer symmetry, and not the crystal symmetry. The former is discussed by R. Zallen, M. L. Slade, and A. T. Ward, *Phys. Rev. B* **3**, 4257 (1971).  
<sup>15</sup>M. E. Sharfe, *Phys. Rev. B* **2**, 5025 (1970); M. D. Tabak and P. J. Warter, Jr., *Phys. Rev.* **173**, 899 (1968).

PHYSICAL REVIEW B

VOLUME 8, NUMBER 4

15 AUGUST 1973

## Pair Spectra and the Shallow Acceptors in ZnSe

J. L. Merz, K. Nassau, and J. W. Shiever  
*Bell Laboratories, Murray Hill, New Jersey 07974*  
 (Received 13 October 1972)

Donor-acceptor pairs associated with the three effective-mass-like donors Al, Ga, and In have been observed in the photoluminescence spectra of ZnSe. The previously determined binding energies of these donors are  $\sim 28$  meV. Under conditions of weak excitation, the distant pair band peaks at an energy of  $\sim 2.69$  eV. The identification of discrete pair lines indicates that both the donor and acceptor are on the same sublattice. The shift of all pair lines by 0.05–0.1 meV to lower energy when crystals are doped with the Li<sup>6</sup> isotope proves that the acceptor is substitutional Li, with a binding energy  $E_A = 114 \pm 2$  meV. A second shallow acceptor, tentatively assigned to Na, has  $E_A \sim 90$ –100 meV, estimated from the corresponding bound-exciton line. Another more complex pair spectrum is reexamined. The discrete pair lines for this system exhibit a doubling of all lines, but the chemical identity of the donor and acceptor producing this spectrum remains undetermined.

### I. INTRODUCTION

The observation and analysis of the many sharp lines appearing in donor-acceptor pair spectra is a powerful tool for understanding the nature of the common donors and acceptors in a compound semiconductor. This recombination process, where an electron on a donor recombines with a hole on an acceptor, was first suggested by Prener and Williams<sup>1</sup> to interpret broad green and red luminescence bands in ZnS. However, detailed evidence for this process was not obtained until the characteristic sharp-line structure resulting from many different discrete pairs was observed and analyzed in GaP.<sup>2,3</sup> The kinetics of pair recombination is now well understood,<sup>4</sup> and a large amount of detailed information about impurities in GaP has resulted from studies of pair spectra.<sup>5-7</sup> Discrete pair lines have also been observed in BP,<sup>8</sup> AlSb,<sup>9</sup> and SiC.<sup>10,11</sup> More recently, pair spectra have also been observed in several II-VI compounds.<sup>12-16</sup>

This paper is the third of a series on the optical properties of ZnSe. In the first<sup>12</sup> (hereafter referred to as DM), analysis of a discrete-line pair spectrum indicated that the donor and acceptor were on the same sublattice, but it could not be determined whether the Zn or Se site was involved, and the impurities responsible were not chemically identified. The second paper<sup>17</sup> (re-

ferred to as MKNS) presented a detailed study of the optical properties of excitons bound to the common simple donors in ZnSe, and the binding energy was determined for five shallow donors: Al, Ga, In, Cl, and F. The present paper is a continuation of the work reported by MKNS. For the three metal-ion donors Al, Ga, and In, pair spectra have been observed with discrete lines. Analysis of these pair lines proves that for each pair both the donor and the acceptor belong to the same sublattice; the acceptor must therefore also be on the Zn site. When crystals are grown in the presence of the Li<sup>6</sup> isotope, the resulting energy shift of the pair lines proves that the acceptor is substitutional Li. Finally, the pair spectrum reported by DM is reexamined in light of the above results, and the differences between this pair system and those involving the three metal ions are discussed.

### II. EXPERIMENTAL

Most of the experimental techniques used in this work have already been described by MKNS. The crystals were grown from the vapor phase using a technique which has previously been described.<sup>18</sup> Crystals were doped with Li and Na by adding the carbonates of these alkali metals to the ZnSe charge, along with excess Zn. Successive growth runs without additional doping are an essential feature of this technique. A few attempts were also